

IMPROVING DETECTION IN SEA CLUTTER USING WAVEFORM SCHEDULING

Sandeep P. Sira[†], Douglas Cochran[†], Antonia Papandreou-Suppappola[†], Darryl Morrell[†],
Bill Moran[‡], Stephen Howard[§], Robert Calderbank^{*}

[†]Arizona State University, [‡]University of Melbourne, [§]DSTO Australia, ^{*}Princeton University

ABSTRACT

In this paper, we propose a method to exploit waveform agility in modern radars to improve performance in the challenging task of detecting small targets on the ocean surface in heavy clutter. The approach exploits the compound-Gaussian model for sea clutter returns to achieve clutter suppression by forming an orthogonal projection of the received signal into the clutter subspace. Waveform scheduling is then performed by incorporating the information about the clutter into the design of the next transmitted waveform. A simulation study demonstrates the effectiveness of our approach.

Index Terms— Clutter, radar detection, signal design

1. INTRODUCTION

The development of waveform-agile sensors provides modern radars with several opportunities to improve performance by dynamic adaptation of the transmitted waveform. For example, in target tracking applications, waveforms can be dynamically selected to obtain target parameter estimates that best contribute to minimizing the tracking error [1–3]. Alternatively, waveform scheduling has been used to minimize the dwell time of the radar on a specific location, reduce ambiguity due to the presence of strong clutter or jamming signals, and classify targets [4, 5].

While waveform design has long been used to mitigate the effect of sea clutter [6], dynamic adaptation does not appear to have been investigated for this purpose. This problem remains relevant and challenging due to the requirement to detect small targets that present low signal-to-clutter ratio (SCR) due to low grazing angles and high sea states. Early investigations generally employed a Gaussian model for the amplitude distribution of sea clutter returns. With the advent of high resolution imaging capabilities, this model failed to predict the observed increased occurrence of higher clutter amplitudes or *spikes*. Instead, the compound-Gaussian (CG) was shown to be a better fit, both theoretically and empirically [7–10].

In this paper, we consider several *snapshots* of the sea surface that are obtained by rapid imaging with a medium pulse-repetition frequency (PRF) radar. Employing the CG model

for sea clutter returns, and assuming that the radar scene can be considered practically stationary over several pulse repetition intervals (PRI), we demonstrate that we can form a waveform-independent estimate of the subspace occupied by the clutter returns. We then form an orthogonal projection of the received signal into this subspace to achieve clutter suppression. When matched filtering is performed at the radar receiver, energy is smeared from one range-Doppler cell to another in accordance with the ambiguity function of the transmitted waveform. To minimize the effect of out-of-bin clutter in a range cell that is to be interrogated (or tested) as a potential target location, we estimate the strength of the clutter in its neighboring cells using the expectation-maximization (EM) algorithm. These estimates are used to design a phase-modulated (PM) waveform whose autocorrelation function is such that it minimizes this smearing effect and improves detection performance.

The paper is organized as follows. In Section 2, we describe the CG model for sea clutter and the processing of the received signal. Section 3 describes the subspace estimation and clutter suppression, while Section 4 presents the details of the dynamic waveform scheduling process. Simulation examples are presented in Section 5.

2. CLUTTER AND SIGNAL MODELS

We consider the radar scene to consist of a number of clutter scatterers and at most one point target, distributed in range and Doppler. Each *dwell* on this scene consists of two sub-dwells, Sub-dwells 1 and 2, during each of which the radar transmits K pulses of the waveforms $s_1(t)$ and $s_2(t)$.

2.1. Compound-Gaussian Model for Sea Clutter

According to the CG model, sea clutter returns are believed to be the result of two components: a speckle-like return generated by a large number of independent scattering centers, and a texture caused by large-scale swell structures that modulates the local mean power of the speckle return [7]. The speckle gives rise to locally Gaussian statistics, characterized by short correlation time (~ 10 ms), while the texture decorrelates much less rapidly (~ 50 s) [7, 8, 10]. The texture component also exhibits spatial correlation and various distributions

This work was supported by the DARPA, Waveforms for Active Sensing Program under NRL grant N00173-06-1-G006.

such as gamma, inverse-gamma, log-normal, or Weibull, have been used to model it. In this paper, we will *not* assume any particular distribution for the texture, as it is not needed for our waveform design.

Assuming that the texture across a range-Doppler cell is constant, we treat all scatterers within the i th cell as a single aggregate scatterer with complex reflectivity over K snapshots $\mathbf{x}_i = [x_i^0, x_i^1, \dots, x_i^{K-1}]^T$. The CG model states that \mathbf{x}_i follows a complex Gaussian probability distribution with zero mean and covariance matrix $\mathcal{T}_i \Sigma$, where $\mathcal{T}_i \geq 0$ is the texture, and $\Sigma \in \mathbb{C}^{K \times K} \neq \mathbb{I}_K$ is the speckle covariance matrix with \mathbb{I}_K denoting the $K \times K$ identity matrix [9]. Given the texture and the speckle covariance matrix, the reflectivities of two scatterers \mathbf{x}_i and \mathbf{x}_j are independent so that

$$p(\mathbf{x}_i, \mathbf{x}_j | \mathcal{T}_i, \mathcal{T}_j, \Sigma) = p(\mathbf{x}_i | \mathcal{T}_i, \Sigma) p(\mathbf{x}_j | \mathcal{T}_j, \Sigma). \quad (1)$$

2.2. Range Processing

With a PRF ~ 10 kHz, the duration of each sub-dwell can be made much smaller than the decorrelation time of the speckle, and we assume that the radar scene is practically stationary during this period. Thus, we assume that the number of scatterers in each cell, and the scatterers' delays and Doppler shifts, are constant during a sub-dwell. However, the scatterer amplitudes x_i^k may fluctuate randomly because small changes in range, on the order of the radar wavelength, may cause significant changes in the phase of the received signal. We will also assume that the texture is fully correlated across a dwell. At the k th pulse, $k = 0, 1, \dots, K - 1$, the received signal is

$$g^k(t) = b^k s(t - \tau_0) e^{j2\pi\nu_0 t} + \sum_i x_i^k s(t - \tau_i) e^{j2\pi\nu_i t} + n(t), \quad (2)$$

where b^k, τ_0 and ν_0 are the complex reflectivity, delay and Doppler shift, respectively, of the target (if present), τ_i and ν_i are the delay and Doppler shift of the i th scatterer, respectively, and $n(t)$ is additive noise. In (2), the transmitted signal $s(t)$ may be $s_1(t)$ or $s_2(t)$ as the processing of the received signal is identical in both sub-dwells. In heavy clutter scenarios, the interference from clutter dominates the effect of the noise, and we will henceforth ignore the latter component. Since we only consider transmitted signals of very short duration, the Doppler resolution is very poor. Therefore, we completely ignore Doppler processing and restrict our attention to delay or range estimation alone.

The received signal in (2) is sampled at a rate f_s to yield a sequence $g^k[n] = g^k(n/f_s)$. This sampled signal is then matched filtered at *each* sampling instant to yield the sequence $r^k[n]$. We define $\mathbf{r}_j \in \mathbb{C}^{K \times 1} = [r^0[j], r^1[j], \dots, r^{K-1}[j]]^T$ as the vector of matched-filtered outputs at the j th delay or range bin. Then,

$$\mathbf{r}_j = \mathbf{b} z_s[j - n_0] + \sum_{n=-(N-1)}^{(N-1)} \mathbf{x}_{j+n} z_s[n], \quad (3)$$

where N is the length of the transmitted signal sequence $s[n]$, and $z_s[m] = \sum_{n=0}^{N-1} s[n] s^*[n - m]$, $|m| < N$, is the value of the autocorrelation function of $s[n]$ at lag m . In (3), n_0 and \mathbf{b} are the range bin and complex reflectivity of the target, respectively.

3. SUBSPACE-BASED CLUTTER SUPPRESSION

To obtain the clutter-suppressed signal, we first obtain an estimate of the clutter subspace for each range bin. To form the subspace estimate \hat{Q}_j of the clutter in the j th range bin, we define a neighborhood Γ_j of range bins with indices $j \pm n$, where $N \leq n < N + N_Q$. The neighborhood Γ_j thus includes $2N_Q$ bins that constitute the training data but does not include any bins that contain contributions from the scatterers in bin j . Thus, the presence of a target in the j th bin does not corrupt the training data used to estimate \hat{Q}_j . Next, we form the covariance matrix

$$\hat{R}_j = \frac{1}{2N_Q} \sum_{n \in \Gamma_j} \mathbf{r}_n \mathbf{r}_n^H, \quad (4)$$

where the superscript H denotes Hermitian transpose. We then perform the eigen-decomposition of \hat{R}_j and define \hat{Q}_j as the subspace spanned by the $N_e < K$ principal eigenvectors of \hat{R}_j . Let \hat{Q}_j^\perp denote the space spanned by the remaining eigenvectors of \hat{R}_j . The orthogonal projection of the received signal in (3) on the clutter subspace \hat{Q}_j is then given by

$$\mathbf{r}_j^\perp = \hat{Q}_j^{\perp H} \mathbf{r}_j, \quad (5)$$

and constitutes the clutter-suppressed signal. From (1), (3), and (4), it can be shown that the waveform dependence of \hat{R}_j in (4) only scales its eigenvalues, thus providing a subspace estimate that is waveform-independent.

4. WAVEFORM SCHEDULING

In order to implement the dynamic design of the waveform, we identify a potential target location, estimate the strength of the clutter in its neighborhood, and design the waveform so that its autocorrelation function satisfies certain constraints.

4.1. Detection

To determine the bin that potentially contains a target, we perform a simple constant-false-alarm-rate (CFAR) detection on \mathbf{r}_j^\perp in (5) at the end of Sub-dwell 1. For this purpose, we first form the test statistic $\gamma_j = \|\mathbf{r}_j^\perp\|_2$, where $\|\cdot\|_2$ denotes the L_2 -norm. For each range bin, a threshold γ_j^{thr} is computed as the average of γ_j in the surrounding bins. The bin in which the ratio $\gamma_j / \gamma_j^{thr}$ is the maximum, is then chosen as the bin to be interrogated in Sub-dwell 2.

4.2. Estimation of Clutter Power

From the CG model, we note that the sea clutter can be expected to be strong where the texture component is large. If the j th range bin is to be interrogated in Sub-dwell 2, to estimate the strength of the clutter, we then require an estimate of the texture values in all bins in the range $[j-(N-1), j+(N-1)]$, excluding bin j itself, since these bins contribute out-of-bin clutter to \mathbf{r}_j . This estimate is obtained via a straightforward application of the EM algorithm [11].

Briefly, we seek an estimate of

$$\boldsymbol{\theta} = \{\mathcal{T}_{j-(N-1)}, \dots, \mathcal{T}_j, \dots, \mathcal{T}_{j+(N-1)}, \boldsymbol{\Sigma}\},$$

that maximizes $p(\mathbf{r}; \boldsymbol{\theta})$, the probability of \mathbf{r} that depends on $\boldsymbol{\theta}$, where $\mathbf{r} = [\mathbf{r}_{j-(N-1)}^T, \dots, \mathbf{r}_j^T, \dots, \mathbf{r}_{j+(N-1)}^T]^T$ is the observed data. Due to the many-to-one mapping in (3), this requires a complicated multi-dimensional search. Using the EM algorithm we instead find an estimate $\hat{\boldsymbol{\theta}}$ that maximizes $p(\mathbf{x}; \boldsymbol{\theta})$, where $\mathbf{x} = [\mathbf{x}_{j-(N-1)}^T, \dots, \mathbf{x}_j^T, \dots, \mathbf{x}_{j+(N-1)}^T]^T$ is the *unobserved* or *complete* data.

4.3. Dynamic Waveform Design

The aim of our waveform design is to minimize the magnitude of the autocorrelation function of the transmitted waveform $s_2(t)$ in Sub-dwell 2, in regions where strong out-of-bin clutter has been estimated from data gathered during Sub-dwell 1. Let $s_2(t)$ represent a unimodular PM waveform given by $s_2(t) = \exp(j\psi(t))$, $0 \leq t \leq T$, where the phase modulation is expanded in terms of an orthogonal set of basis functions as $\psi(t) = \sum_{i=1}^M \lambda_i \psi_i(t)$, and $\psi_i(t) = u(t - (i-1)\Delta T_s) - u(t - i\Delta T_s)$, where $u(t)$ is the unit step function that is unity except for $t < 0$ [12]. Here, the total waveform duration $T = M\Delta T_s$ and $M \leq N$, where N is the number of samples in the designed signal. We want to determine the coefficients λ_i that minimize the integral of the squared magnitude of the autocorrelation function over the range of τ values for which the clutter is estimated to be strong. With the autocorrelation function of $s_2(t)$ defined as $z_{s_2}(\tau)$, we seek to minimize

$$J(\boldsymbol{\lambda}) = \int_{Z_\tau} |z_{s_2}(\tau)|^2 d\tau, \quad (6)$$

where $\boldsymbol{\lambda} = [\lambda_1, \lambda_2, \dots, \lambda_M]^T$, and Z_τ represents the (possibly disconnected) set of range values for which the texture values are large. It is relatively straightforward to show that

$$\begin{aligned} z_{s_2}(\tau) &= (\Delta T_s - \Delta\tau) \sum_{i=1}^{M-m} \exp\{j(\lambda_{m+i} - \lambda_i)\} \\ &+ \Delta\tau \sum_{i=1}^{M-m-1} \exp\{j(\lambda_{m+i-1} - \lambda_i)\} \end{aligned}$$

where $|\tau| = m\Delta T_s + \Delta\tau \leq T$, $m \leq M-1$, and $0 \leq \Delta\tau < \Delta T_s$. Using the squared magnitude of $z_{s_2}(\tau)$, the gradient and Hessian of $J(\boldsymbol{\lambda})$ can be easily computed and its

minimization can be accomplished by the Newton-Raphson method. All that remains is to choose the set Z_τ , which is accomplished by selecting the bins that have the $N_t < 2(N-1)$ largest estimated texture values. Note that the evaluation of $J(\boldsymbol{\lambda})$ in (6) reduces to a discrete summation in this scenario.

5. SIMULATIONS

Our simulation model consists of a target that is observed by a single sensor in the presence of simulated K -distributed sea clutter. Accordingly, texture variables are sampled from a gamma distribution and correlated by passing them through a linear filter. In order to have a realistic speckle covariance matrix, we estimated the autocorrelation function of the speckle component from experimental clutter data, collected at the Osborne Head Gunnery Range (OHGR) with the McMaster University IPIX radar [13]. In each sub-dwell, $K = 10$ pulses of a $1.5 \mu\text{s}$ duration signal are transmitted. The waveform $s_1[n]$ is a linear frequency modulated (LFM) chirp with a frequency sweep of 50 MHz and it was ensured that $s_2[n]$ did not exceed the time-bandwidth product of $s_1[n]$ so that a fair comparison could be made. The PRI is $100 \mu\text{s}$ so that the duration of each sub-dwell is 1 ms, which is well within the decorrelation time of the speckle component, while the sampling frequency was $f_s = 100$ MHz. The number of eigenvectors N_e of the covariance matrix in (4) that contribute to the subspace estimate were chosen so that 99.99% of the total energy was retained, and a neighborhood of $N_Q = 20$ bins was used to obtain the subspace estimates. The amplitude of the target return \mathbf{b} in (3) was sampled from a zero mean complex Gaussian process with covariance matrix $\sigma^2 \mathbb{I}_K$, where σ^2 was chosen to satisfy specified values of SCR. We define the SCR to be the ratio of the target signal power to the *total* power of the clutter in the range bin containing the target.

Fig. 1 shows Monte Carlo averaged receiver operating characteristic (ROC) curves when only subspace-based clutter suppression is used. Since no dynamic waveform design has been employed, these curves represent the performance at the end of Sub-dwell 1. The advantage of using the clutter suppression procedure described in Section 3 is significant, and Fig. 1 indicates reasonable performance even at low SCR such as -35 dB. This can be primarily attributed to the fact that the clutter occupies a low-rank subspace of the covariance matrix of the received signal.

The advantages of waveform design can be seen in Fig. 2, where the ROC curves at the end of Sub-dwell 2 (in which the dynamically designed waveform is transmitted) are compared with those at the end of Sub-dwell 1. We observe that the performance improves further when the waveform is adapted to the clutter. Specifically, the ROC curve for -28 dB SCR at the end of Sub-dwell 2 is comparable to the ROC curve for -25 dB SCR at the end of Sub-dwell 1. Also, at a probability of false alarm $P_{FA} = 0.01$, the probability of detection P_D improves by 20% and 25% at SCR of -28 dB and -25 dB, respectively, when the designed waveform is used. This improvement is

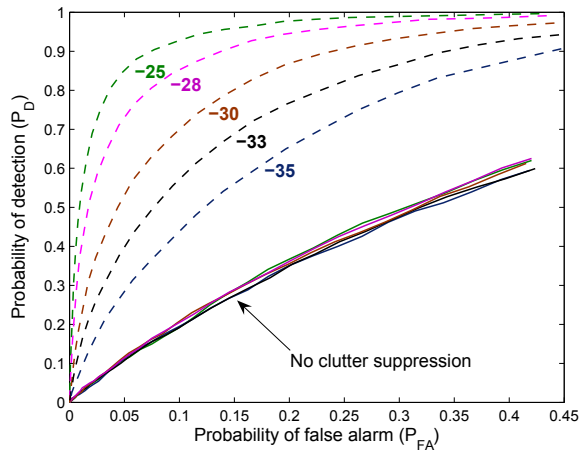


Fig. 1. ROC curves with (dotted lines) and without (solid lines) clutter suppression using a static LFM chirp waveform. The indicated values correspond to SCR in dB.

due to the fact that the waveform design procedure described in Section 4 provides a reduction of upto 30 dB in autocorrelation magnitude in range bins where the clutter is estimated to be strong.

6. CONCLUSION

We have presented an automatic waveform scheduling algorithm that employs subspace-based clutter suppression and dynamic waveform design to improve target detection in heavy sea clutter. The method exploits the CG model for sea clutter returns and designs waveforms with autocorrelation functions which have small magnitude where the clutter is estimated to be strong. Simulation results demonstrate that significant improvements in detection performance are obtained by clutter suppression while further gains are made by the introduction of waveform scheduling. In recent work, we have demonstrated greater performance gains due to waveform scheduling by replacing the CFAR detector with a generalized likelihood ratio test (GLRT) detector [14]. We are currently in the process of including of Doppler processing in our work. Note that this is not a straightforward extension because the need for longer waveforms to achieve high Doppler resolution may invalidate the assumption of complete correlation of the texture across a dwell.

7. REFERENCES

- [1] S. D. Howard, S. Suvorova, and W. Moran, "Waveform libraries for radar tracking applications," *Int. Conf. on Waveform Diversity and Design*, Nov. 2004.
- [2] S. P. Sira, A. Papandreou-Suppappola, and D. Morrell, "Characterization of waveform performance in clutter for dynamically configured sensor systems," *Waveform Diversity and Design Conf.*, Jan. 2006, Lihue, Hawaii.
- [3] S. P. Sira, A. Papandreou-Suppappola, and D. Morrell, "Dynamic configuration of time-varying waveforms for agile sens-

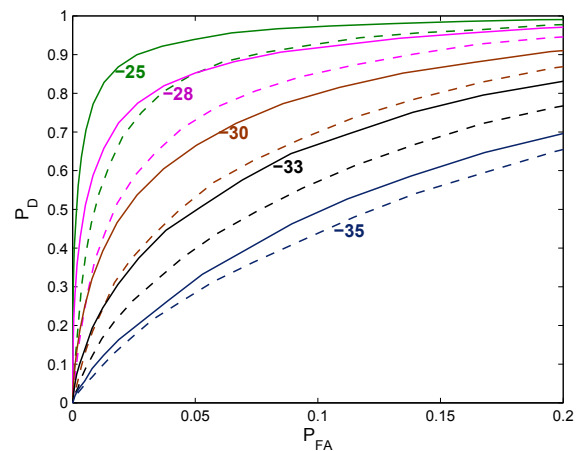


Fig. 2. ROC curves when dynamic waveform design (solid lines) and a static LFM chirp (dotted lines) are used.

ing and tracking in clutter," *IEEE Trans. Signal Processing*, Accepted.

- [4] B. F. La Scala, W. Moran, and R. J. Evans, "Optimal adaptive waveform selection for target detection," in *International Conference on Radar*, 2003, pp. 492–496.
- [5] S. M. Sowelam and A. H. Tewfik, "Waveform selection in radar target classification," *IEEE Trans. Inform. Theory*, vol. 46, pp. 1014–1029, May 2000.
- [6] D. F. DeLong and E. M. Hofstetter, "On the design of optimum radar waveforms for clutter rejection," *IEEE Trans. Inform. Theory*, vol. IT-13, no. 3, pp. 454–463, Jul. 1967.
- [7] S. Haykin, R. Bakker, and B. W. Currie, "Uncovering nonlinear dynamics - The case study of sea clutter," *Proc. IEEE*, vol. 90, pp. 860–881, May 2002.
- [8] K. D. Ward, C. J. Baker, and S. Watts, "Maritime surveillance radar Part I : Radar scattering from the ocean surface," *IEE Proc. F*, vol. 137, no. 2, pp. 51–62, Apr. 1990.
- [9] K. J. Sangston and K. R. Gerlach, "Coherent detection of radar targets in a non-Gaussian background," *IEEE Trans. Aerosp. Electron. Syst.*, vol. 30, no. 2, Apr. 1994.
- [10] A. Farina, F. Gini, M. V. Greco, and L. Verrazzani, "High resolution sea clutter data: statistical analysis of recorded live data," *IEE Proc. on Radar, Sonar and Navigation*, vol. 144, no. 3, pp. 121–130, Jun. 1997.
- [11] M. Feder and E. Weinstein, "Parameter estimation of superimposed signals using the EM algorithm," *IEEE Trans. Acoust., Speech, Sig. Proc.*, vol. 36, pp. 477–489, Apr. 1988.
- [12] J. D. Wolf, G. M. Lee, and C. E. Suyo, "Radar waveform synthesis by mean-square optimization techniques," *IEEE J. Oceanic Eng.*, vol. AES-5, no. 4, pp. 611–619, Jul. 1969.
- [13] A. Drosopoulos, "Description of the OHGR database," Tech. Rep. 94-14, Def. Research Establishment, Ottawa, Dec. 1994.
- [14] S. P. Sira, A. Papandreou-Suppappola, D. Morrell, D. Cochran, W. Moran, S. Howard, and R. Calderbank, "Adaptive waveform design for improved detection of low-RCS targets in heavy sea clutter," *IEEE Journal on Special Topics in Sig. Proc.: Special Issue on Adaptive Waveform Design for Agile Sensing and Communication*, Jun. 2007, In review.